Electronic Supplementary Information

One-pot synthesis of a highly active, non-spherical PdPt@Pt core-shell nanospike electrocatalyst exhibiting a thin Pt shell with multiple grain boundaries

Jisun Yoon,[a+] *Sungwon Kang,*[a+] *Hionsuck Baik,*[*b] *Yong Soo Choi,*[c] *Seong Jung Kwon,*[*c] *and Kwangyeol Lee*[*a]

[a] Department of Chemistry and Research Institute for Natural Sciences, Korea University, Seoul 136-701 (Korea)

[b] Korea Basic Science Institute (KBSI), Seoul 136-713 (Korea)

[c] Department of Chemistry, Konkuk University, Seoul 143-701 (Korea)

[+] These authors contributed equally.

*Corresponding authors: kylee1@korea.ac.kr (K. Lee), sjkwon@konkuk.ac.kr (S. J. Kwon), baikhs@kbsi.re.kr (H. Baik)

Material Characterizations

Transmission electron microscopy (TEM) and high-resolution TEM (HRTEM) were performed on a TECNAI G2 20 S-Twin operated at 200kV and TECNAI G2 F30 operated at 300 kV. Elemental mapping and energy dispersive X-ray spectra (EDX) were obtained with a JEOL ARM200F Cs STEM. X-ray diffraction (XRD) patterns were collected with a Rigaku Ultima III diffractometer system using a graphite-monochromatized Cu-Kα radiation at 40kV and 40mA. The electrochemical experiment was performed using a CHI model 660d potentiostat (CH Instruments, Austin, TX).

Experimental Section

Preparation of Pd_mPt_n nanostructures (Fig. 3)

A slurry of $Pt(acac)_2$ (Aldrich, 97%), $Pd(acac)_2$ (Strem, 99%), octadecylamine (Aldrich, 97%), stearic acid (Aldrich, 95%), 1,2-hexadecanediol (Aldrich, 90%), and trioctylphosphine (Aldrich, 90%) was prepared in a two-neck bottom flask (25 mL) with a magnetic stirring. The flask was heated to 90 ^oC placed in the oil bath, and then evacuated for 5 min with magnetic stirring, and finally purged with Ar gas. Resulting reaction mixture was placed in an oil bath preheated to 180 ^oC, and was heated for 1h at that temperature. Dark brownish precipitates were obtained as products after introducing toluene into the cooled reaction mixture, centrifugation, and washing several times with methanol.

The synthetic conditions are summarized in the table shown below. The elemental ratios were obtained from EDX analysis. (Fig.S4-9)

	$Pt(acac)_2$	$Pd(acac)_2$	Trioctylphosphine	Octadecylamine	Stearic acid	1,2-Hexadecanediol
$Pd_{0.65}Pt_{0.35}$ alloy	0.05 mmol	0.05 mmol	0.11 mmol	7.4 mmol	1 mmol	100 mg
$Pd_{0.56}Pt_{0.44}$ alloy	0.05 mmol	0.05 mmol	0.11 mmol	7.4 mmol	8 mmol	100 mg
$Pd_{0.52}Pt_{0.48}$ alloy	0.2 mmol	0.05 mmol	0.11 mmol	7.4 mmol	1 mmol	100 mg
$Pd_{0.32}Pt_{0.68}$ core-shell	0.2 mmol	0.05 mmol	0.11 mmol	7.4 mmol	8 mmol	100 mg
$Pd_{0.41}Pt_{0.59}$ alloy	0.285 mmol	0.05 mmol	0.11 mmol	7.4 mmol	1 mmol	100 mg
$Pd_{0.17}Pt_{0.83}$ core-shell	0.285 mmol	0.05 mmol	0.11 mmol	7.4 mmol	8 mmol	100 mg

Electrochemical experiment and instruments

Pt/C (20 %(w/w) Pt on Vulcan XC72) was purchased from Aldrich and used for reference. (Glassy carbon electrodes (GCE) (dia. 3 mm, CH Instruments, Austin, TX) purchased and used as support for PdPt nanostructures. GCEs were prepared and polished with alumina powder (dia. 1.0 and 0.3 μm) on a polishing pad (Buehler) followed by sonication in diluted water for 5 min. Electrodes were washed with water and dried (30 min). In order to place nanostructures on GCE, 10 μL of 1/100 diluted Nafion® perfluorinated ion-exchange resin solution (5 % (w/w) in lower aliphatic alcohols/water mix, Aldrich) was applied on the cleaned GCE and dried for 30 min. 5.5 mg of prepared $Pd_{0.65}Pt_{0.35}$ alloy, 3.6 mg of prepared $Pd_{0.32}Pt_{0.68}$ core-shell, 5.1 mg of prepared $Pd_{0.17}Pt_{0.83}$ core-shell, 2.3 mg of prepared $Pd_{0.56}Pt_{0.44}$ alloy, 2.3 mg of prepared $Pd_{0.41}Pt_{0.59}$ alloy, or 2.3 mg of prepared $Pd_{0.52}Pt_{0.48}$ alloy were dispersed in 2 mL of toluene each. Then, 10 μL of each PdPt nanostructure stock solution was dropped on the nafion® pre-coated GCE and dried for 24h in room temperature. The electrochemical experiment was performed by CHI model 660d potentiostat (CH Instruments, Austin, TX). The three-electrode electrochemical cell consisting of a Hg/Hg_2SO_4, K_2SO_4 (sat'd) reference electrode (0.64 V vs. NHE), a modified by nafion® GC working electrode and an Au wire counter electrode. All the potential values in this paper were converted as reporting vs. NHE.

Oxygen Reduction Reaction (ORR) was performed in a 0.5 M H_2SO_4 solution (saturat'd O_2 or Ar). Methanol Oxidation Reaction (MOR) was performed in a solution containing 0.5 M methanol and 0.5 M H_2SO_4. The nanostructure modified GCE was electrochemically cleaned before the measurement, by scanning the potential between -0.7 V to 1.0 V (19 cycles) in a 0.5 M H_2SO_4 solution, in order to remove surface impurities in PdPt nanostructures.

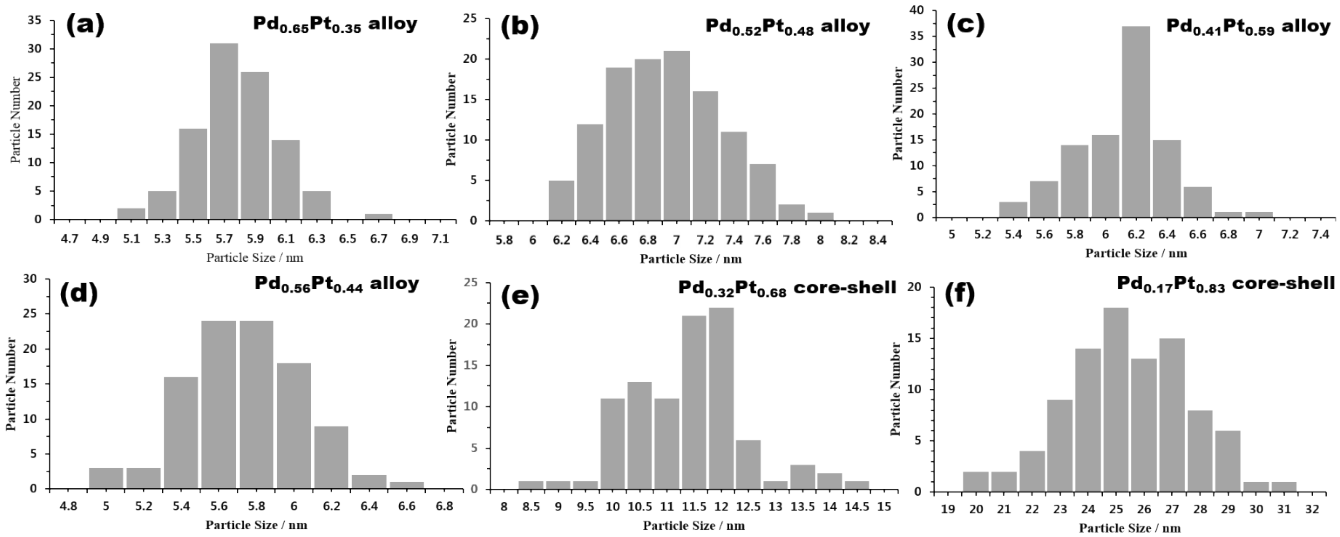

Fig. S1 Size distributions for (a) $Pd_{0.65}Pt_{0.35}$ alloy, (b) $Pd_{0.52}Pt_{0.48}$ alloy, (c) $Pd_{0.41}Pt_{0.59}$ alloy, (d) $Pd_{0.56}Pt_{0.44}$ alloy, (e) $Pd_{0.32}Pt_{0.68}$ core-shell and (f) $Pd_{0.17}Pt_{0.83}$ core-shell by counting 100 nanoparticles in each case. The average size: (a) 5.8 nm (± 0.3) of $Pd_{0.65}Pt_{0.35}$ alloy, (b) 6.9 (± 0.4) nm of $Pd_{0.52}Pt_{0.48}$ alloy, (c) 6.2 nm (± 0.3) of $Pd_{0.41}Pt_{0.59}$ alloy, (d) 5.7 nm (± 0.4) of $Pd_{0.56}Pt_{0.44}$ alloy, (e) 11.5 (± 1.1) nm of $Pd_{0.32}Pt_{0.68}$ core-shell, and (f) 25.5 (± 2.1) nm of $Pd_{0.17}Pt_{0.83}$ core-shell.

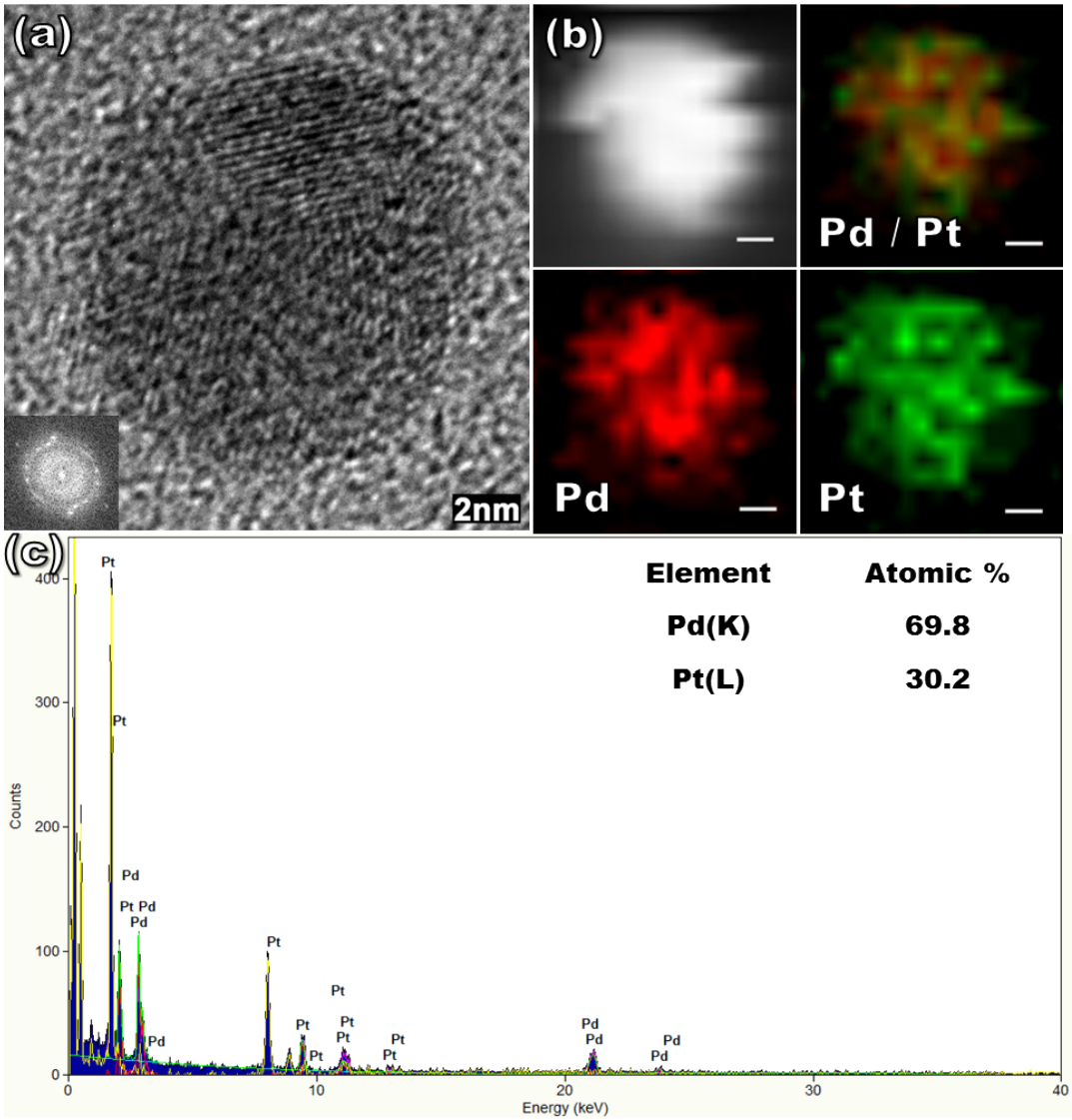

Fig. S2 (a) HR-TEM image, (b) STEM image, elemental mapping and (c) EDX data of a nanoparticle in fig. 2c. (a) HR-TEM image shows that the nanoparticle has multiple crystal domains, as indicated by the corresponding FFT image in Inset. (b) Pd and Pt phases are thoroughly mixed to form a random alloy. The scale bar in (b) is 2 nm.

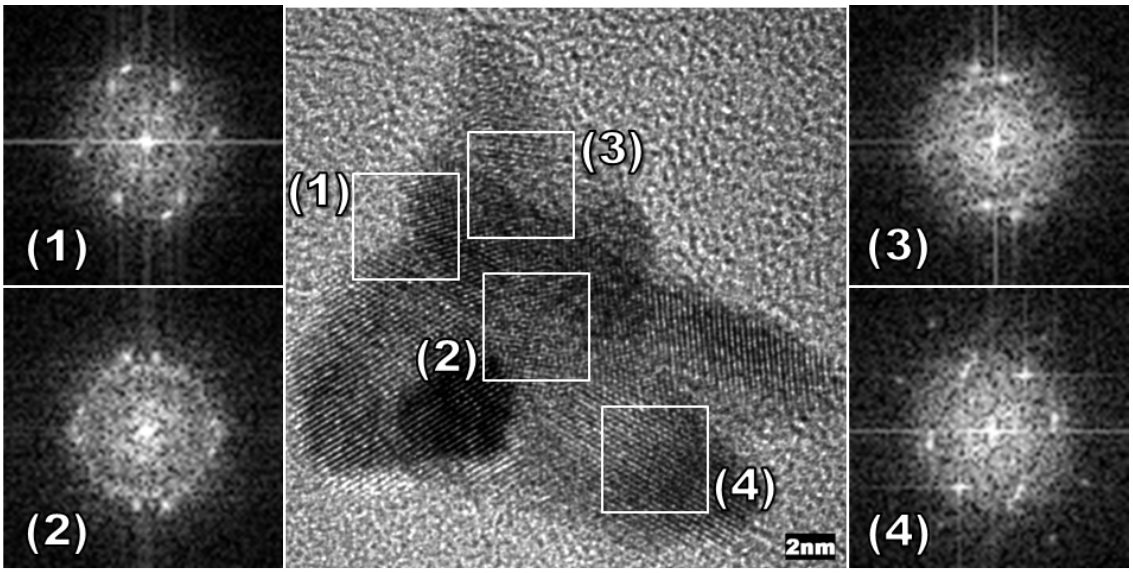

Fig. S3 HR-TEM image and FFT patterns of a $Pd_{0.17}Pt_{0.83}$ core-shell in Fig. 3i, 3l. (1-4) The corresponding FFT patterns show a high crystalinity and multiple grain boundaries in the Pt shell. The central part shows a poor crystallinity.

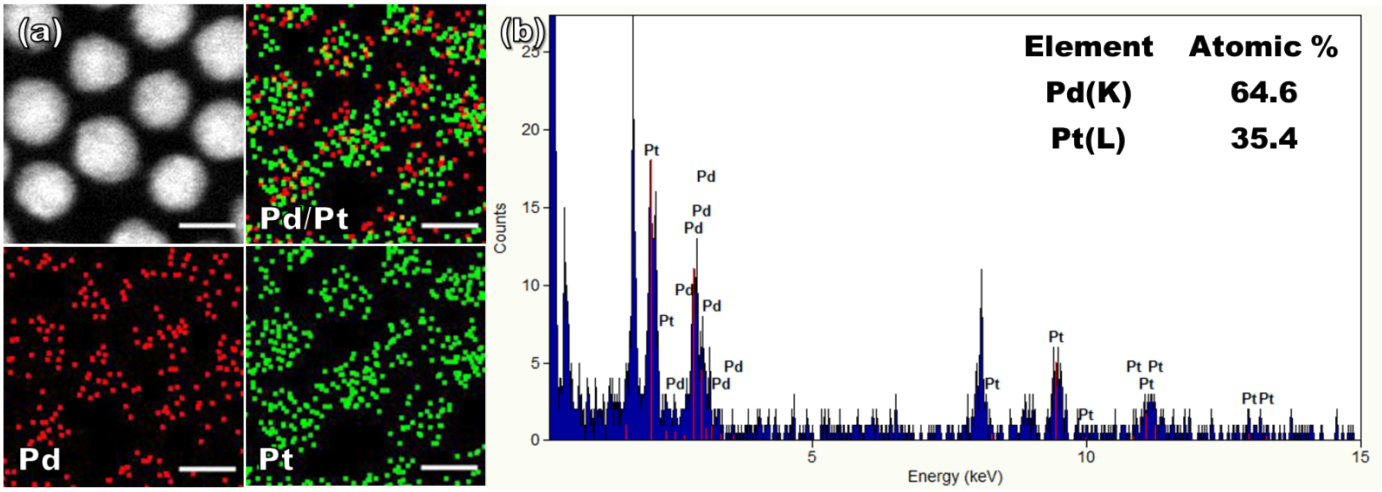

Fig. S4 (a) STEM, elemental mapping analysis and (b) EDX data of $Pd_{0.65}Pt_{0.35}$ alloy in Fig. 3a, 3d. The scale bar in (a) is 5 nm.

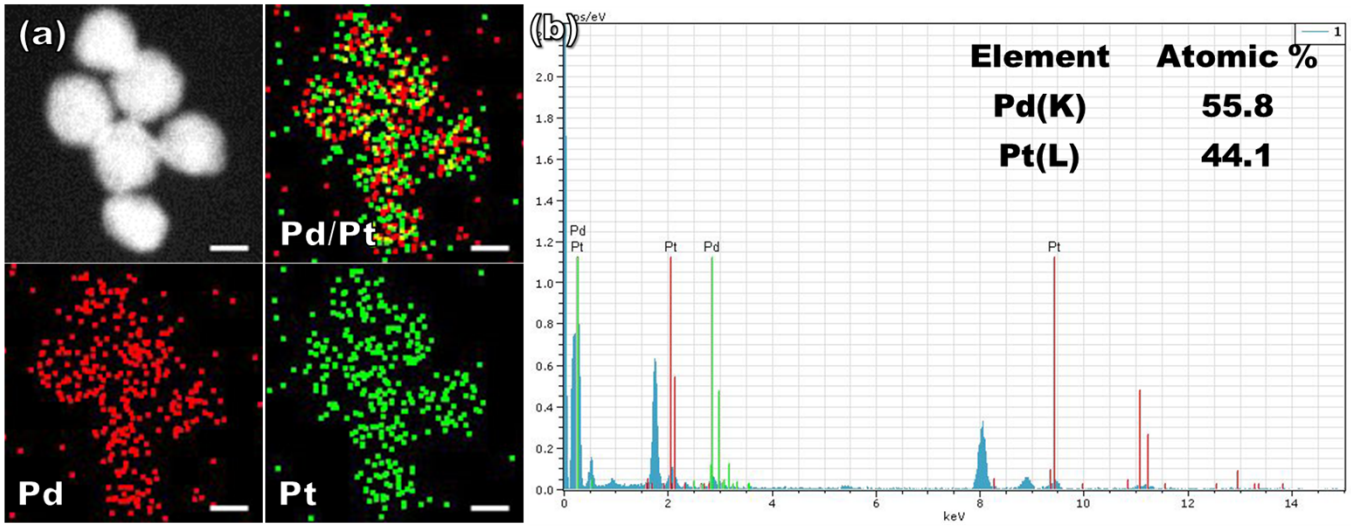

Fig. S5 (a) STEM, elemental mapping analysis and (b) EDX data of $Pd_{0.56}Pt_{0.44}$ alloy in Fig. 3g, 3j. The scale bar in (a) is 5 nm.

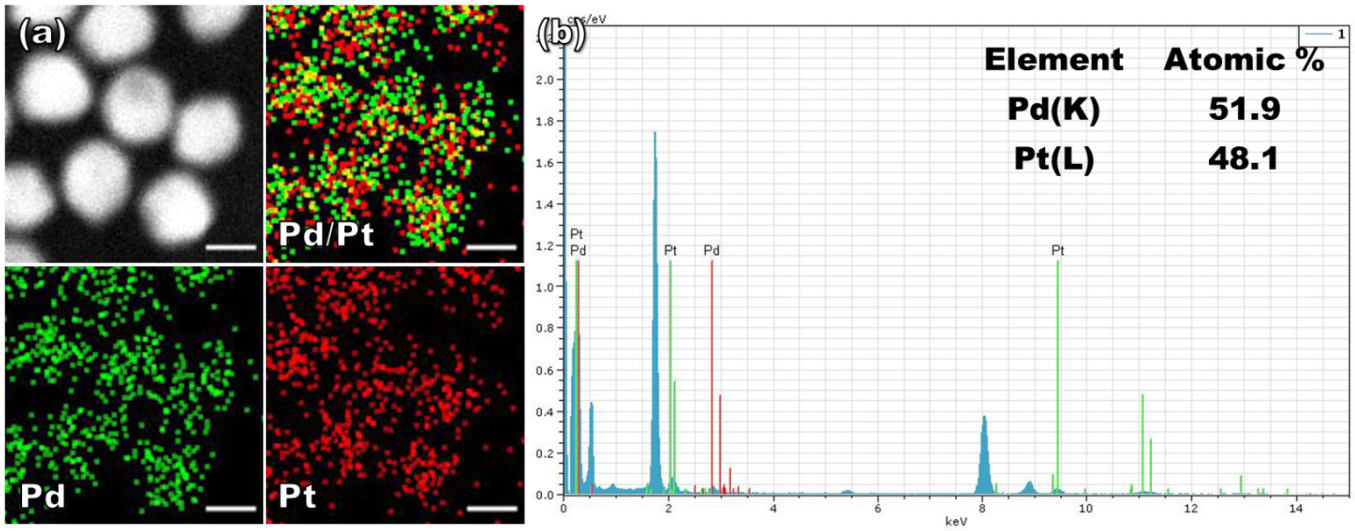

Fig. S6 (a) STEM, elemental mapping analysis and (b) EDX data of $Pd_{0.52}Pt_{0.48}$ alloy in Fig. 3b, 3e. The scale bar in (a) is 5 nm.

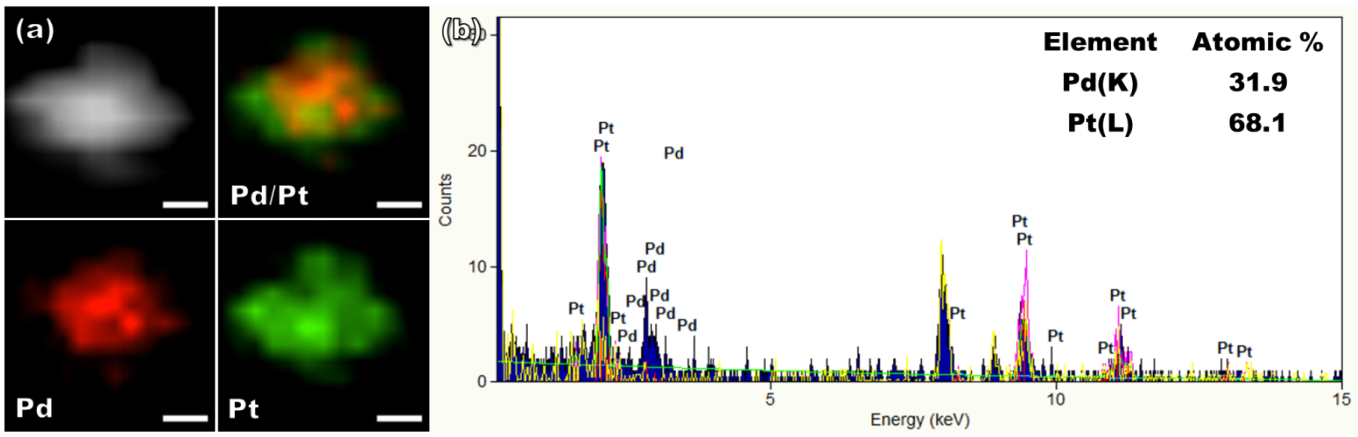

Fig. S7 (a) STEM, elemental mapping analysis and (b) EDX data of $Pd_{0.32}Pt_{0.68}$ core-shell in Fig. 3h, 3k. The scale bar in (a) is 3 nm.

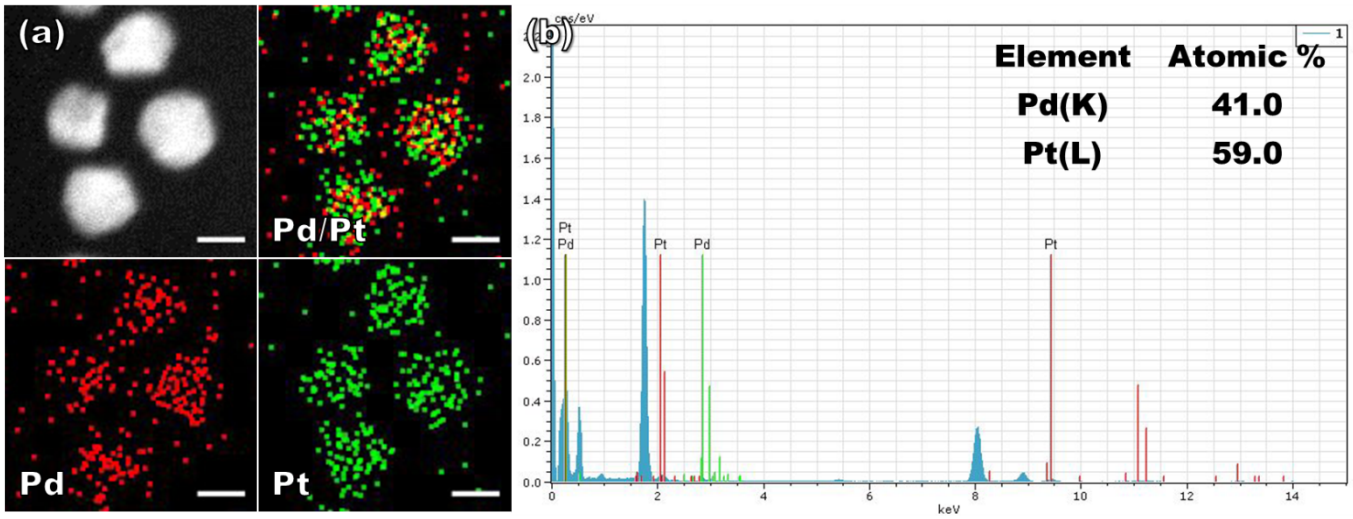

Fig. S8 (a) STEM, elemental mapping analysis and (b) EDX data of $Pd_{0.41}Pt_{0.59}$ alloy in Fig 3c, 3f. The scale bar in (a) is 5 nm.

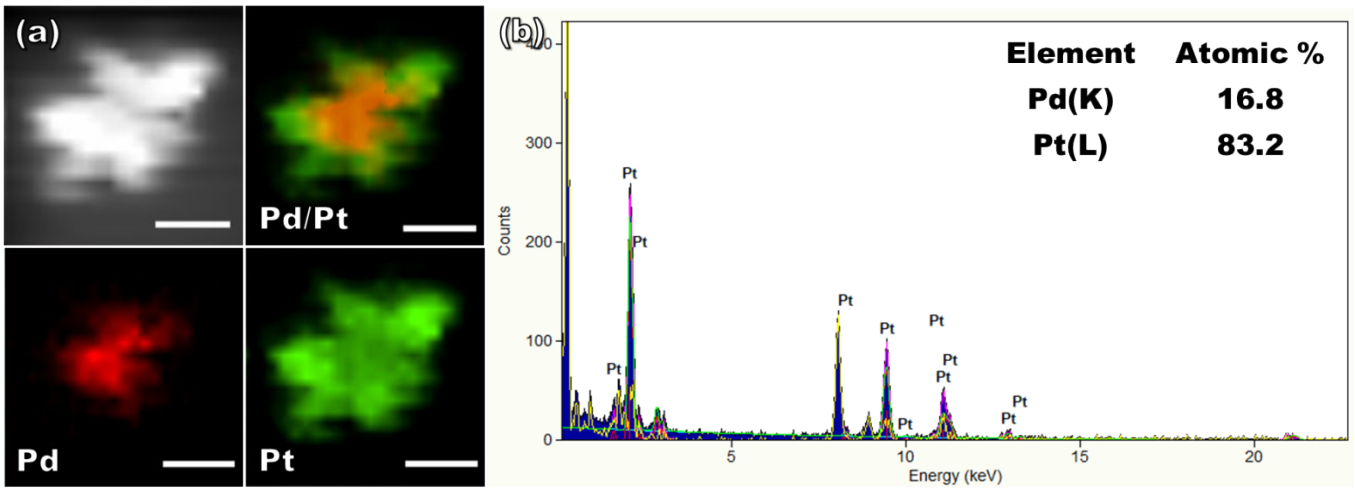

Fig. S9 (a) STEM, elemental mapping analysis and (b) EDX data of $Pd_{0.17}Pt_{0.83}$ core-shell in Fig. 3i, 3l. The scale bar in (a) is 10 nm.

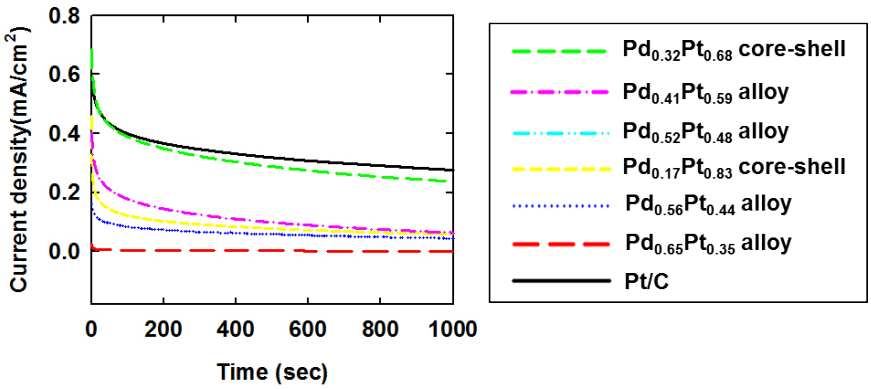

Fig. S10 Chronoamperometry curves of commercial Pt/C and PdPt nanostructures-modified glassy carbon electrodes (GCEs) in 0.5 M MeOH + 0.5 M H_2SO_4 electrolyte solution. Scan rate was 50 mV/s.

Nanostructure	ECSA(m^2/g)	Forward scan		Backward scan	
		Current density (mA/cm^2)	Mass activity (mA/mg)	Current density (mA/cm^2)	Mass activity (mA/mg)
$Pd_{0.65}Pt_{0.35}$ alloy	20.7	0.024	5.06	0.0052	1.08
$Pd_{0.52}Pt_{0.48}$ alloy	4.68	0.390	18.3	0.286	13.4
$Pd_{0.41}Pt_{0.59}$ alloy	4.15	0.677	28.1	0.565	23.5
$Pd_{0.56}Pt_{0.44}$ alloy	8.51	0.319	27.1	0.272	23.1
$Pd_{0.32}Pt_{0.68}$ core-shell	216	0.901	1946	1.02	2199
$Pd_{0.17}Pt_{0.83}$ core-shell	10.6	0.335	35.5	0.255	27.0
Pt/C	250	0.670	1737	0.771	1998

Table. S1 Electrocatalytic properties of commercial Pt/C and PdPt nanostructures for MOR

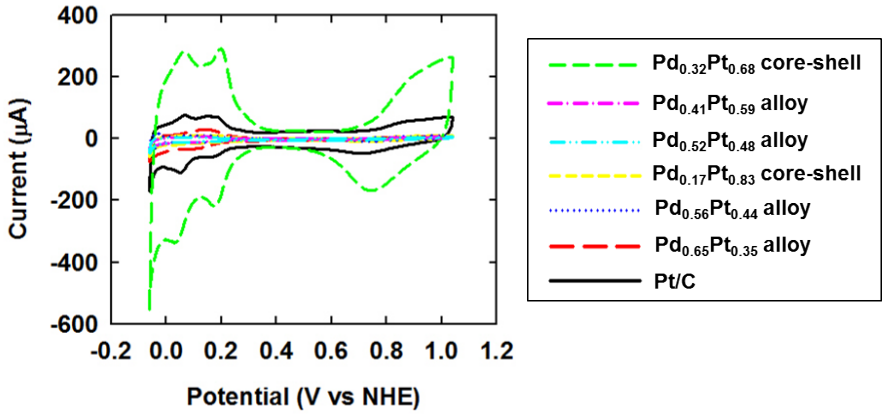

Fig. S11 Cyclic voltammograms of Pt/C and PdPt nanostructures-modified GCE in Ar-saturated 0.5 M H_2SO_4 electrolyte solution. Scan rate was 50 mV/s.

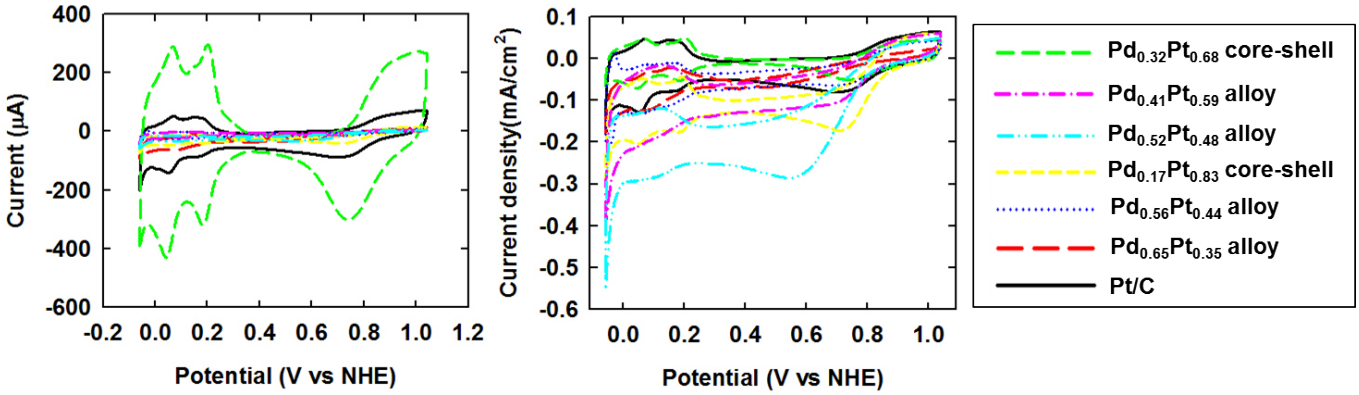

Fig. S12 Cyclic voltammograms of Pt/C and PdPt nanostructures-modified GCE in O_2-saturated 0.5 M H_2SO_4 electrolyte solution expressed by (a) current and (b) current density. Scan rate was 50 mV/s.

Nanostructure	ECSA (m^2/g)	Current density (mA/cm^2)	Mass activity (mA/mg)
$Pd_{0.65}Pt_{0.35}$ alloy	8.38	0.069	5.77
$Pd_{0.52}Pt_{0.48}$ alloy	4.68	0.271	12.7
$Pd_{0.41}Pt_{0.59}$ alloy	4.15	0.095	3.96
$Pd_{0.56}Pt_{0.44}$ alloy	8.51	0.064	5.44
$Pd_{0.32}Pt_{0.68}$ core-shell	151	0.050	76.1
$Pd_{0.17}Pt_{0.83}$ core-shell	4.18	0.172	7.20
Pt/C	250	0.080	201

Table. S2 Electrocatalytic properties of Pt/C and PdPt nanostructures for ORR.

Estimation of electrochemically active surface area (ECSA)

The CVs obtained at the Ar atmosphere (Fig. S10) were used for the estimation of ECSA of the synthesized PdPt nanostructures. Generally, the ECSA of Pt based catalyst was determined by measuring the charge collected in the hydrogen adsorption/desorption region after double-layer correction and assuming a value of (210 μC/cm^2), the charge needed for oxidation of a single layer of hydrogen on a smooth Pt surface.[1] However, the method to estimated ECSA is different in the case of Pd base catalyst. The ECSA of the Pd electrodes was measured by determining the coulombic charge (Q) for the reduction of palladium oxide. The charge required for the reduction of PdO monolayer is assumed as 405 mC/cm^2.[2] Unfortunately, we could not find any distinguishable Pd oxide peak in our PdPt nanostructures. Therefore, the general method for the estimation of ECSA of Pt catalyst based on the hydrogen adsorption/desorption was still applied for the estimation of ECSA of PdPt nanostructures.[3]

Electrocatalytic activity for oxygen reduction reaction (ORR)

The electro-catalytic property of PdPt nanostructures toward oxygen reduction reaction (ORR) is also investigated by CV. The $Pd_{0.32}Pt_{0.68}$ alloy nanoparticle shows enormous improvement in the ECSA. Due to the large ECSA, the current density was relatively smaller than the others. (Note: the current density of $Pd_{0.32}Pt_{0.68}$ alloy is still huge for the MOR.) Therefore, the $Pd_{0.52}Pt_{0.48}$ alloy nanoparticle shows the best ORR activity.

The current densities, the mass activity, and the electrochemically active surface areas (ECSA), determined by the hydrogen desorption method, were calculated toward ORR and are shown in Table S2.

Reference

1. S. Trasatti and O. A. Petrii, *Pure Appl. Chem.,* 1991, **63,** 711.
2. T. Biegler, D. A. J. Rand and R. Woods, *J. Electroanal. Chem.,* 1971, **29,** 269.
3. H-H. Li, S. Zhao, M. Gong, C-H. Cui, D. He, H-W. Liang, L. Wu and S-H. Yu, *Angew. Chem. Int. Ed.*, 2013, **52**, 7472.